The Micro-Hole-and-Strip Plate Gas Detector: Experimental Results

J. M. Maia, J. F. C. A. Veloso, R. E. Morgado, J. M. F. dos Santos, and C. A. N. Conde

***Abstract*—We report the performance characteristics of a new microstructure, the micro-hole-and-strip plate (MHSP), operated initially as an X-ray proportional counter. The MHSP combines the features of a microstrip plate (MSP) and a gas electron multiplier (GEM) in a single microstructure. Like the GEM, the MHSP is fabricated using flexible printed circuit board technology. The MHSP provides two independent charge-amplification stages: a first stage consisting of slotted holes, operated as a GEM, and a second stage, the MSP anodes, that also function as the final charge-collection electrodes. Two obvious benefits accrue from this design: for a given total gain, the MSP anode-to-cathode voltage can be maintained well below the breakdown threshold and the charge-amplification stages are optically isolated, in anticipation of future applications as a photosensor. Full electron transmission and total gains up to 1000 were achieved, with slotted-hole gains as high as 14. The best energy resolution achieved thus far for 5.9-keV X-rays is 23%. Measurements of gains, electron transmission, and energy resolution, as functions of biasing voltages, are reported.**

***Index Terms*—Gas electron multiplier, microstrip gas chamber.**

I. Introduction

SINCE the introduction of the micro-strip gas chamber (MSGC) in 1988 [1], microstructures with different geometries produced by photolithographic methods on insulating substrates have been investigated. The primary motivation is to develop radiation gas detectors for tracking systems in the next generation of high-energy-physics collider experiments. In all cases, amplification is derived from a charge avalanche in the intense electric field near the micro-strip (MS) anodes at voltages near the limit of electrical breakdown.

More recently, the gas electron multiplier (GEM) [2] based on flexible printed circuit board technology was introduced. GEMs are arrays of sub-millimeter holes etched through a thin polymer substrate with isolated conductors deposited on each side. Charge amplification occurs in the avalanche produced when electrons are accelerated through the intense electric field within the holes. GEMs usually require an additional charge-amplification/charge-collection stage, frequently a microstrip plate (MSP).

Manuscript received November 23, 2001; revised February 13, 2002. This work was supported by Project POCTI/43527/99. The work of R. E. Morgado was supported by the Gulbenkian Foundation and the Foundation for Luso-American Development (FLAD). The work of J. F. C. A. Veloso was supported by Fundação para a Ciência e a Tecnologia (FCT).

J. M. Maia is with the Physics Department, University of Beira Interior, P-6201-001 Covilhã, and also with the Physics Department, University of Coimbra, P-3004-516 Coimbra, Portugal.

J. F. C. A. Veloso, J. M. F. dos Santos, and C. A. N. Conde are with the Physics Department, University of Coimbra, P-3004-516 Coimbra, Portugal (e-mail: jveloso@gian.fis.uc.pt).

R. E. Morgado is with Los Alamos National Laboratory, Los Alamos, NM 87545 USA.

Publisher Item Identifier S 0018-9499(02)06152-X.

A new microstructure, the micro-hole- and -strip plate (MHSP) [3], [4], was conceived as a combination of the features of the MSP and the GEM in a single microstructure. Like the GEM, the MHSP can be fabricated using flexible printed circuit board (PCB) technology. As designed, the MHSP provides two independent charge-amplification stages: the slotted holes, operated as a GEM (first stage); and the MS anodes (second stage), which also function as charge-collection electrodes. By dividing the gain between two stages, MS anode-to-cathode voltages can be well below the breakdown threshold while the total gain is already adequate for X-ray spectroscopy in a gas detector.

By optically isolating the two gain stages, we hope to eliminate the limitation of positive optical feedback in a future application of the MHSP as a photosensor. Photosensors based on microstructures that operate within the gas envelope of a proportional scintillator counter have great appeal for applications that require compact and rugged radiation sensors capable of operation in high magnetic fields [5]. Our previous investigations of photosensors based on microstructures [6] showed that positive optical feedback resulted when the UV light produced in the avalanches in one region is viewed directly by a photocathode surface. This effect limits the gain to values too low for useful photosensors.

Prior to investigating the future prospects of the MHSP as a photosensor, we evaluated its fundamental operating characteristics as a charge-amplifying system. We present the experimental results of the first of a series of first-generation MHSP designs operated as a proportional counter for detecting X-rays.

II. Description

The MHSP was fabricated with advanced flexible PCB technology (Fig. 1). Limitations in present photolithographic technology [7] required a compromise between the original design specifications and what was realizable in practice. Consequently, we believe our present results, although promising, represent the minimum performance characteristics of the design and can be markedly improved with a second-generation MHSP that not only matches the specifications of the original design [3] more closely but also provides higher quality etching uniformity and reproducibility.

The MHSP dimensions are shown in Fig. 2. Both sides of a 25 μm Kapton polymer substrate are deposited with 5-μm —thick copper films. A standard microstrip pattern of anodes and cathodes is etched onto one side [the MS side, Fig. 1(b)] while the reverse side is initially featureless. The widths of the MS anodes and cathodes are 56 and 224 μm, respectively, with a 420-μm pitch. Then, 112-μm-wide slotted holes are etched through the MS cathodes to the front side [Fig. 1(a)] leaving 56-μm-wide cathodes on each border of the slotted hole. The

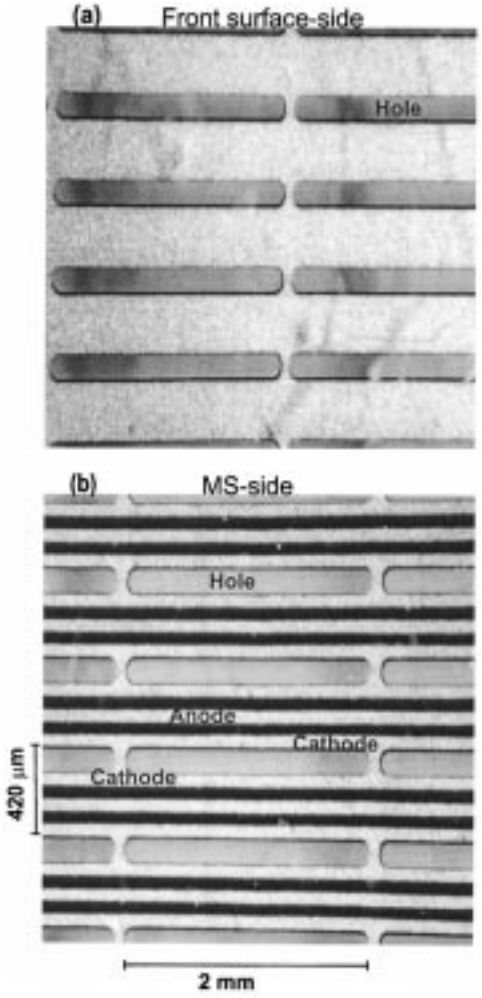

Fig. 1. Photomicrographs of (a) the front surface side and (b) the MS side of an MHSP.

total active area is 4.5×5.0 cm^2. For structural integrity of the microstructure, the slotted holes were limited to 2 mm in length.

III. Operation

To establish baseline operational characteristics for the MHSP, it was operated as a gas proportional counter. Other modes of operation, including the primary motivation as a UV photosensor in a gas proportional scintillation counter, will be considered in future works.

A detector schematic is depicted in Fig. 2. The MHSP structure is mounted on a frame located between two parallel conductors that comprise the entrance window and the back surface of the detector. There are two 3-mm drift regions: d_1, between the entrance window and the front surface of the MHSP, and d_2, between the MHSP and the back surface of the detector.

Variable bias voltages are established between several structures of the MHSP:

- V_{d1} in the drift region between the entrance window and the MHSP front surface;
- $V_{\rm hole}$ between the MHSP front surface and the MS cathodes;
- $V_{\rm ac}$ between the cathodes and anodes of the MS;
- V_{d2} in the drift region between the MS cathodes and the back surface of the detector.

When operated as a proportional counter, the entrance window and the back surface of the detector are biased negatively with respect to the MHSP.

A schematic of some field lines within the detector are shown in Fig. 3. X-rays of energy E_x interact by the photoelectric effect primarily in the 3-mm drift region, d_1, to produce a cloud of N_e primary electrons

$$N_e = \frac{E_x}{w} \tag{1}$$

where w is the w-value of the fill gas.

The primary electron cloud drifts toward the MHSP slotted holes under the influence of the electric field E_{d1} established by V_{d1}. As the cloud approaches the MHSP, the electric field established by $V_{\rm hole}$ accelerates it through the slotted holes. If the field is sufficiently intense to establish the conditions for an avalanche, a charge gain, $G_{\rm hole}$, is obtained. The electrons emerge on the other side of the MHSP and are directed toward the MS anode under the combined influences of $V_{\rm ac}$, $V_{\rm hole}$, and V_{d2}.

At the anode, the charge is further amplified resulting in a total gain G_1

$$G_1 = G_{\rm hole} \times G_2 \tag{2}$$

where G_2 is the gain of the MS anode. The total gain is a function of the several biasing voltages and the fill gas.

A fraction of the incident X-rays will interact in the 3-mm drift region, d_2, below the MHSP. The primary electron clouds from these events will only experience one stage of charge multiplication, G_2, at the MS anode resulting in pulses of correspondingly smaller amplitude These two distinctly different events enable the determination of the gain due to the slotted holes $G_{\rm hole}$ as

$$G_{\rm hole} = \frac{G_1}{G_2}. \tag{3}$$

X-rays from a ^{55}Fe source ($\sim 87\%$ 5.9 keV, $\sim 13\%$ 6.5-keV X-rays), collimated to 2-mm diameter, were used throughout this work. The collected charge from the anodes was integrated and preamplified in a Canberra 2006 charge-sensitive preamplifier (1.5 V/pC), linearly amplified with a Tennelec TC243 linear amplifier (4 μs shaping-time constant, gains $=$ 100 or 200) and pulse-height analyzed in a 1024-multichannel analyzer (MCA). The experimental system was calibrated to allow absolute charge-gain determinations.

The detector was filled with high purity argon, xenon, P-10 and argon/xenon mixtures at a pressure $p = 800$ Torr (106 kPa) and continuously purified by convection through SAES ST707 getters.

For peak-amplitude and energy-resolution determinations, pulse-height distributions were fit to a Gaussian superimposed on a linear background.

IV. Experimental Results and Analysis

A. Fill Gas Mixtures

The first task was to determine a fill-gas mixture that would provide the highest gain in the MS for the lowest applied voltage $V_{\rm ab}$ between the MHSP front surface and the MS anodes. This voltage is the sum of the voltages $V_{\rm hole} + V_{\rm ac}$. In the present

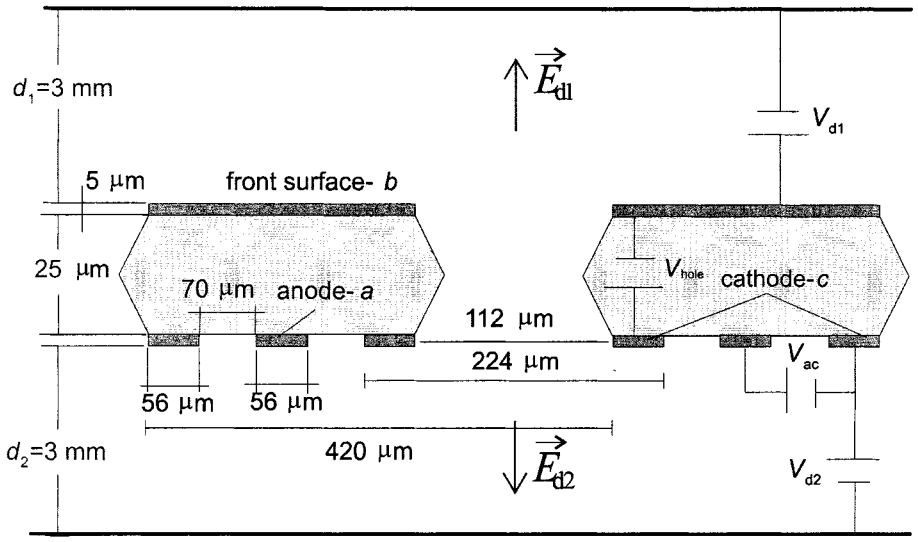

Fig. 2. Schematic of the MHSP-based detector.

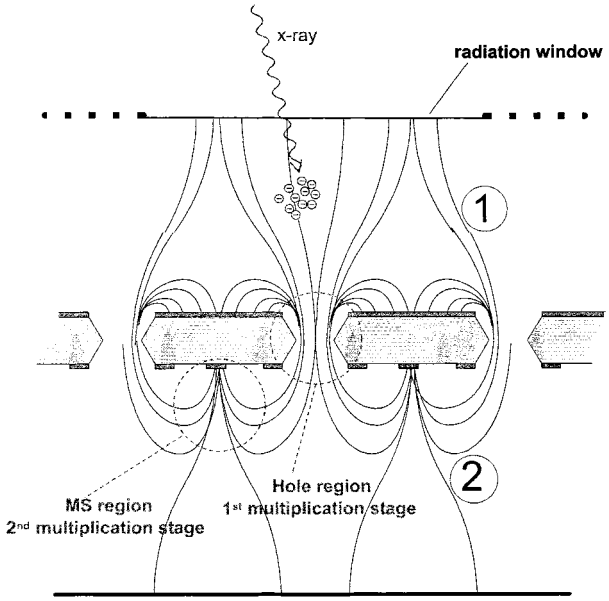

Fig. 3. A schematic of few field lines present within the detector.

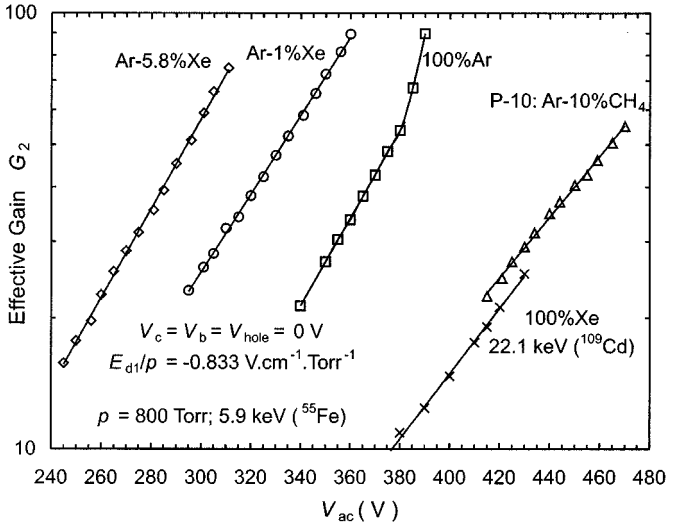

Fig. 4. Gain G_2 as a function of $V_{\rm ac}$ voltage for $V_{\rm hole} = 0$ V and for different gas mixtures.

design, the MHSP substrate thickness and the quality of the etching limit the total sustainable voltage between the MHSP front surface and the MS anode to around 500 V. Consequently, a lower value for the MS anode-to-cathode voltage, $V_{\rm ac}$, for a given gain, G_2, allows the difference, $V_{\rm hole}$, to be applied in the hole region. This was necessary due to the poor etching quality, the large MS anode, and the small gap between MS anodes and cathodes which all combined to limit the attainable MS gain prior to the onset of breakdown.

The method to determine the best gas mixture involved measuring the MS gain, G_2, as a function of $V_{\rm ac}$ with $V_{\rm hole} = 0$ V.

The results for the fill gases that were considered in this study are shown in Fig. 4. The solid lines are intended to serve only as a guide to the eye. For each mixture, $V_{\rm ac}$ was increased until the pulse-height distribution becomes distorted due to microdischarges. The experimental data illustrate the characteristic exponential variation of charge avalanche processes in MSPs. However, positive feedback is noticeable in pure argon for $V_{\rm ac}$ voltages above 380 V. A mixture of Ar-5.8% Xe was determined to be the best choice from among those studied.

By operating the MS with $V_{\rm ac} = 280$ V, a gain G_2 of approximately 35 was achieved.

Having selected an appropriate fill gas, attention could then turn to determining the best performance characteristics as a function of the several adjustable bias voltages.

B. MHSP Effective Gains

The slotted-hole gain as a function of $V_{\rm hole}$ is determined by taking the ratio of the total gain, G_1, for events absorbed above the MHSP to the gain, G_2, for events absorbed below the MHSP (3). The results for all three gains are plotted in Fig. 5 for the bias voltages indicated. We note that the gain G_2 also increases with $V_{\rm hole}$ since the voltage difference between the front electrode and the anode strips has an effect on the field intensity at the MS anode, an effect already described for MSGC [8]. Gains of approximately 12, 75, and 900 can be reached for the hole, MS, and MHSP total gain, respectively, with stable operation.

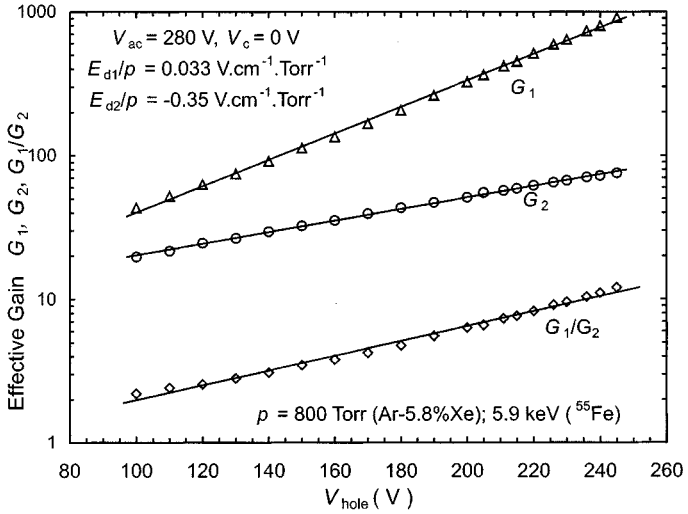

Fig. 5. Effective gains G_1, G_2, and $G_{\rm hole}$ as a function of the voltage $V_{\rm hole}$ for the Ar-5.8% Xe mixture.

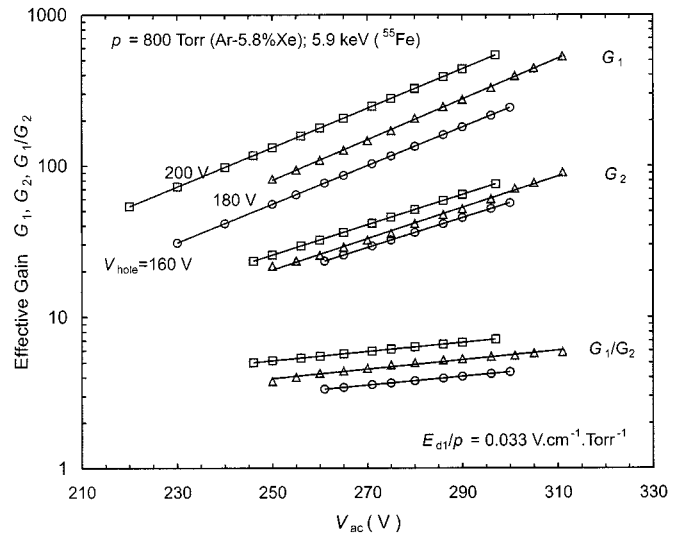

Fig. 6. Effective gains G_1, G_2, and $G_{\rm hole}$ as a function of the voltage $V_{\rm ac}$ for different $V_{\rm hole}$ voltage values and for the Ar-5.8% Xe mixture.

Hole gains as high as ~ 14 were measured, limited only by the maximum value of the sum of $V_{\rm hole} + V_{\rm ac}$ that can be sustained across the 25-μm polymer substrate.

In Fig. 6, the total gain (G_1), MS gain (G_2), and hole gain ($G_{\rm hole}$) are depicted as functions of $V_{\rm ac}$ for different $V_{\rm hole}$ values. As expected, an exponential trend is observed in all cases. Additionally, the behavior exhibited by the total gain curves for the different $V_{\rm hole}$ values indicates that MHSP electron transmission is independent of $V_{\rm ac}$ for the ranges of $V_{\rm ac}$ and $V_{\rm hole}$ studied. The slight increase of $G_{\rm hole}$ with $V_{\rm ac}$, for constant $V_{\rm hole}$, is due to the increase of the electric field intensity in the hole exit region, an effect similar to the increase of the electric field with $V_{\rm ac}$ at the cathode surface of an MSP.

C. Energy Resolution

Fig. 7 shows the pulse-height distribution of 5.9-keV X-rays measured with an Ar-5.8% Xe mixture at 800 Torr for the bias voltages indicated. The salient spectral features include:

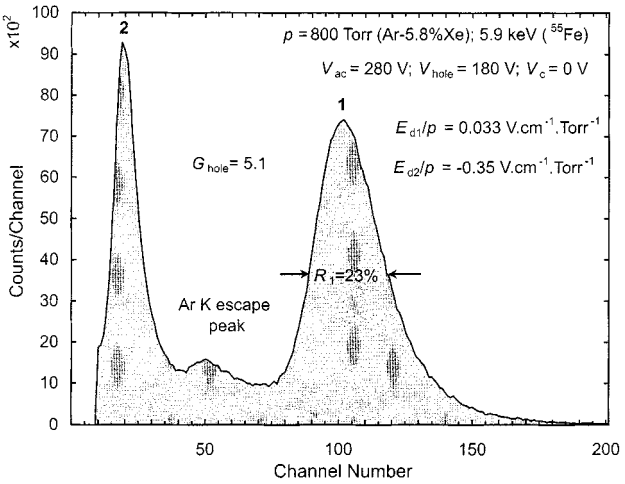

Fig. 7. Typical pulse-height distribution of ^{55}Fe X-rays obtained for $V_{\rm ac} = 280$ V and $V_{\rm hole} = 180$ V and for the Ar-5.8% Xe gas mixture.

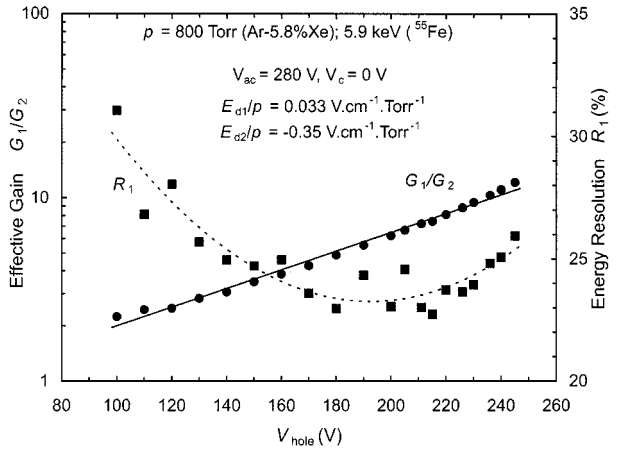

Fig. 8. Energy resolution R_1 and effective gain $G_{\rm hole}$ as a function of $V_{\rm hole}$ for the Ar-5.8% Xe gas mixture.

- a full-energy peak (#1) from 5.9-keV X-rays absorbed in the upper drift region of the detector;
- a smaller peak (#2) from 5.9-keV X-rays absorbed in the lower drift region of the detector for which charge multiplication occurs only at the MS anodes;
- an Ar K-fluorescence escape peak.

The gain in the MHSP slotted holes can be deduced from the ratio of the pulse amplitudes of peak-1 and peak-2. For the bias voltages indicated in Fig. 7, a gain of 5.1 is attributed to the slotted holes alone. The SNR and energy resolution for peak-1 are 35 and 23% while for peak-2 they are 7 and 33%, respectively.

The variation in energy resolution as a function of $V_{\rm hole}$ is plotted in Fig. 8. The best energy resolution for the present MSHP design and quality of fabrication was 23% at 5.9 keV. Further increases in hole gain lead to deterioration of the resolution, likely due to field-emission micro-discharges that increase the statistical fluctuations in the multiplication process. Other limitations on the energy resolution are attributed to nonuniformities in the structure of the anodes, cathodes, and holes as a result of the fabrication process. Nevertheless, at this stage of development, this value compares favorably with the 15% value obtained with a standard gas proportional counter.

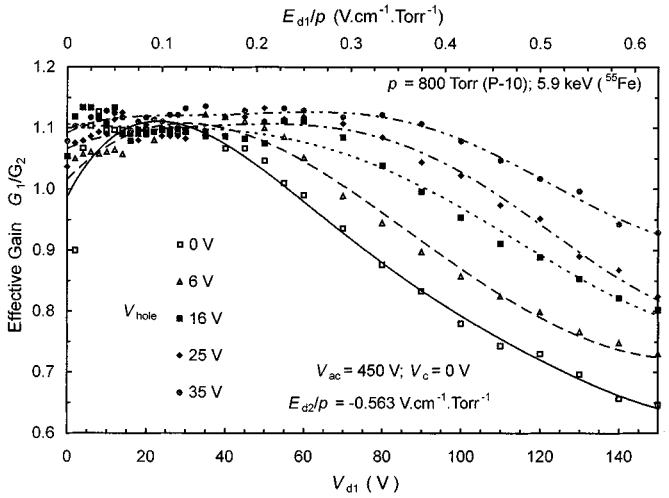

Fig. 9. G_1/G_2 ratio as a function of the V_{d1} for different $V_{\rm hole}$ values and for a P-10 gas mixture.

D. MHSP Electron Transmission

The electron transmission of the MHSP holes was studied as a function of V_{d1}, $V_{\rm hole}$ and $V_{\rm ac}$. Transmission was determined by comparing pulse amplitudes for absorption events that occur above (gain G_1) and below (gain G_2) the MHSP. Since the amplitudes for X-rays absorbed below the MHSP (G_2) are not affected by electron transmission through the slotted holes, the G_1/G_2 ratio is a measure of the MHSP electron transmission for $V_{\rm hole}$ values below the onset of multiplication.

For values of $V_{\rm hole}$ below the multiplication threshold, the centroids of the pulse-height distributions for each type of event need to be determined by subtraction since they both occur with approximately the same amplitude and are not resolvable. To do this, the field in the drift region above the MHSP, E_{d1}, was set to a negative value guaranteeing no transmission through the slotted holes. This allows the centroid for events that occur below the MHSP be determined without interference. These events, normalized to the same data acquisition time, are then subtracted from the pulse-height distribution obtained when the field in the upper drift region is set to its nominal value. The centroid for events that occur above the MHSP is then determined from the difference of the two distributions.

1) Dependence on V_{d1} : An optimum value of V_{d1} was first chosen by investigating the G_1/G_2 ratio as a function of V_{d1} for several values of $V_{\rm hole}$ below the multiplication threshold (Fig. 9). For this study, P-10 gas was chosen for its higher ionization threshold (Fig. 4). Fig. 9 shows a maximum transmission plateau that increases with $V_{\rm hole}$. Maximum transmission is reached for $V_{d1} \sim$ 8–30 V at $V_{\rm hole} = 0$ V and for $V_{d1} \sim$ 2–80 V at $V_{\rm hole} = 35$ V. The same trend is also observed for GEMs [5]. Intuitively, maximum transmission is established when the pulse amplitudes for events above and below the MHSP are approximately equal for $G_{\rm hole} = 1$. In reality, absorption events above the MHSP are known to experience slightly higher multiplications at the MS as a result of their different trajectories, as predicted by simulations [9], [10]. At still higher values of V_{d1}, the MHSP electron transmission decreases due to the increasing loss of primary electrons to the MHSP front surface electrode.

2) Dependence on $V_{\rm hole}$: The data in Fig. 10 depict the G_1/G_2 ratio as a function of $V_{\rm hole}$ for (a) Ar-5.8% Xe and

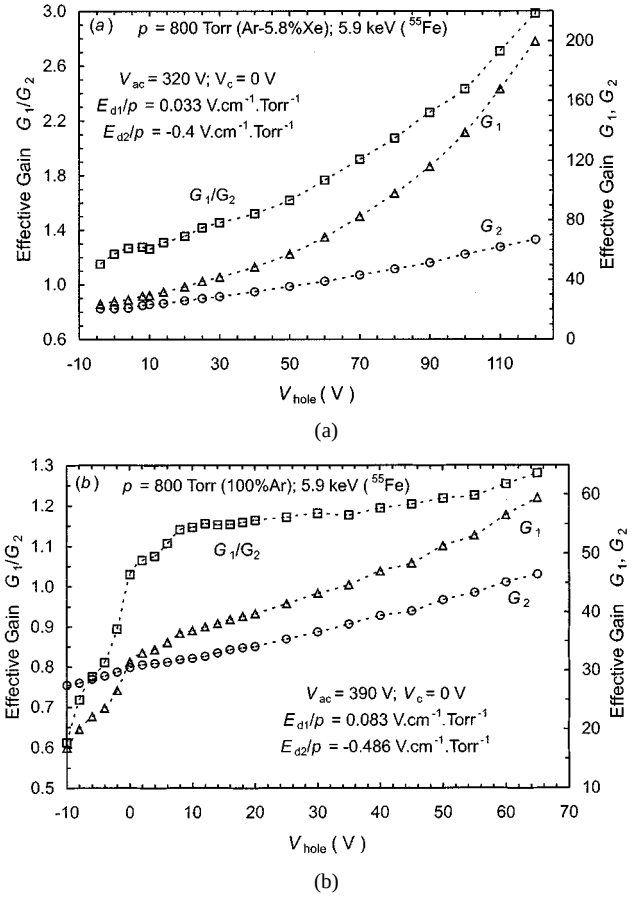

Fig. 10. G_1/G_2 ratio as a function of the $V_{\rm hole}$ for (a) Ar-5.8% Xe gas mixture and (b) pure argon.

(b) pure argon gas fillings. A maximum transmission is achieved at $V_{\rm hole}$ values as low as 5 and 10 V with a plateau extending up to approximately 15 and 35 V for each mixture, respectively. As expected, the plateau is larger for filling gases with higher ionization thresholds.

The dominating influence of the MS anode voltage, $V_{\rm ac}$, on transmission is apparent as good transmission is achieved even for $V_{\rm hole} = 0$ V.

At still higher values of $V_{\rm hole}$, exponential behavior is observed indicating the onset of charge amplification in the hole. The dependence of electron transmission on $V_{\rm ac}$ is insignificant as shown by the results depicted in Fig. 6. A change in the electron transmission with $V_{\rm ac}$ would result in a departure from the exponential dependence exhibited by G_1.

E. Operational Dependence on V_{d2}

We studied the variation of the detector response as a function of the reduced field in the drift region behind the MHSP by varying the voltage V_c. Choosing a suitable electric field E_{d2} in this region can effectively eliminate pulses due to X-ray interactions in the d_2 drift region. However, an electric field that drives primary electrons away from the MS electrodes may also have a deleterious effect on the pulse-height distribution of the X-ray interactions that occur in the region above the MHSP, and this effect required further investigation.

In Fig. 11, we present the results of the relative gains of G_1 and G_2, normalized to $V_c = 0$ V, as a function of V_c for several

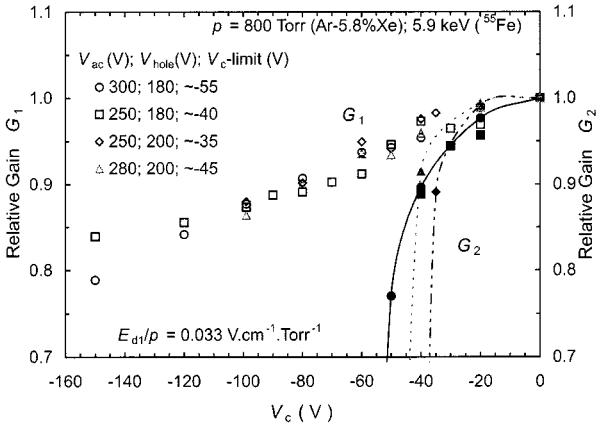

Fig. 11. Relative gains G_1 and G_2, normalized to $V_c = 0$ V, as a function of V_c for several different values of $V_{\rm ac}$ and $V_{\rm hole}$.

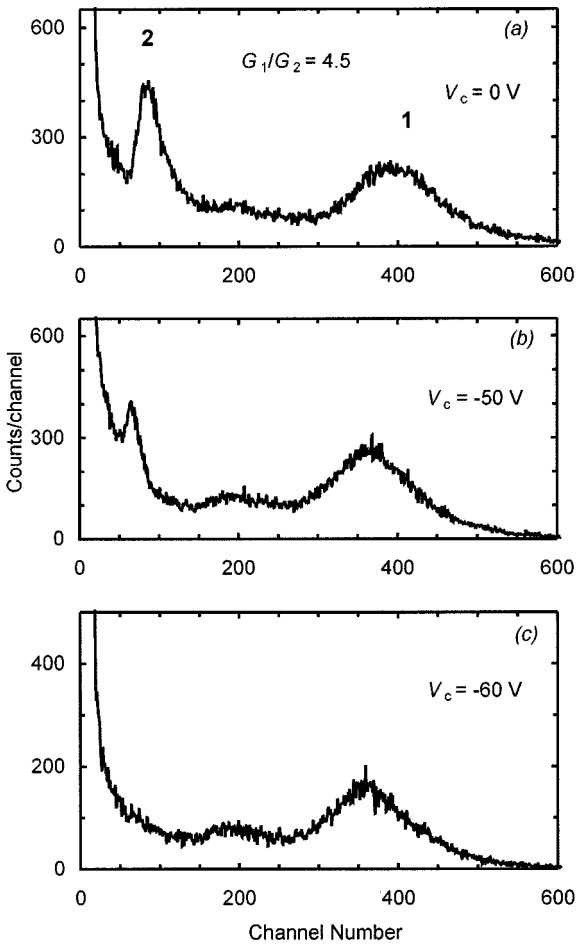

Fig. 12. Pulse-height distributions for 5.9 keV X-rays and an Ar-5.8% Xe gas mixture at $p = 800$ Torr, with $V_{\rm ac} = 300$ V, $V_{\rm hole} = 180$ V and $E_{d1}/p = 0.033$ V.cm^{-1}.Torr^{-1}, for three different V_c voltages: (*a*) $V_c = 0$ V, (*b*) $V_c = -40$ V and (*c*) $V_c = -60$ V.

different values of $V_{\rm ac}$ and $V_{\rm hole}$. The pulse amplitudes of X-ray interactions in the d_2 drift region is seen to decrease rapidly with V_c, eventually disappearing below the noise level at a limiting value V_c that increases with $V_{\rm ac}$ and decreases with $V_{\rm hole}$. Pulse-height distributions for the $V_{\rm ac} = 300$ V, $V_{\rm hole} = 180$ V at three different V_c voltages are shown in Fig. 12. We note that the elimination of pulses resulting from X-ray interactions in the d_2 drift region is achieved with less than 5% reduction in G_1, i.e., in the pulse amplitudes for X-ray interactions above the MHSP.

V. Conclusion

The operational characteristics of the MHSP have been demonstrated. Hole and total gains of 12 and 900, respectively, are achieved with stable operation. Maximum electron transmission through the slotted holes is achieved at nominal operational settings. A minimum energy resolution of $\sim 23\%$ is achieved at 5.9 keV for $G_{\rm hole} \sim 6$.

It was shown that by selecting appropriate values of E_{d2} the drift region behind the MHSP can be rendered insensitive to X-rays absorbed in it without affecting the overall performance of the MHSP.

The limitations in present photolithographic technology required a compromise between what was specified in the original design and what could be realized in practice. Consequently, we believe our results, although promising, represent the minimum performance characteristics of the design and can be markedly improved with a second-generation MHSP that not only matches the specifications of the original design more closely but also exhibits a higher quality of etching uniformity and reproducibility.

Other modes of operation, including the primary motivation as a UV photosensor, will be considered in future work.

Acknowledgment

This work was carried out in the Atomic and Nuclear Instrumentation Group of the Instrumentation Centre (Unit 217/94), Physics Department, University of Coimbra.

References

[1] A. Oed, "A position sensitive detector with microstrip anode for electron multiplication with gases," *Nucl. Instrum. Methods*, vol. A 263, pp. 351–359, 1988.

[2] F. Sauli, "GEM: A new concept for electron amplification in gas detectors," *Nucl. Instrum. Methods*, vol. A 386, pp. 531–534, 1997.

[3] J. F. C. A. Veloso, J. M. F. dos Santos, and C. A. N. Conde, "A proposed new microstructure for gas radiation detectors: The microhole and strip plate," *Rev. Sci. Instrum.*, vol. 71, pp. 2371–2376, 2000.

[4] J. F. C. A. Veloso, J. M. Maia, R. E. Morgado, J. M. F. dos Santos, and C. A. N. Conde, "The micro-hole- and -strip plate gas detector: Initial results," Rev. Sci. Instrum., vol. 73, pp. 488–490, 2002.

[5] S. Bachmann, A. Bressan, L. Ropelewski, F. Sauli, A. Sharma, and D. Mormann, "Charge amplification and transfer processes in the gas electron multiplier," *Nucl. Instrum. Methods*, vol. A 438, pp. 376–408, 1999.

[6] J. F. C. A. Veloso, J. M. F. dos Santos, C. A. N. Conde, F. Mulhauser, P. Knowles, C. Donche-Gay, O. Huot, D. Taqqu, and F. Kottmann, "Driftless gas proportional scintillation counter for muonic hydrogen X-ray spectroscopy under strong magnetic fields," *Nucl. Instrum. Methods*, vol. A 460, pp. 297–305, 2001.

[7] Tech-Etch, Inc., Plymouth, MA, 02360, USA.

[8] F. Angelini, R. Bellazzini, L. Bosisio, A. Brez, M. M. Massai, G. Spandre, and M. R. Torquati, "A microstrip chamber on a silicon substrate," *Nucl. Instrum. Methods*, vol. A 314, pp. 450–454, 1992.

[9] D. S. A. P. Freitas, J. F. C. A. Veloso, J. M. F. dos Santos, and C. A. N. Conde, "A comparative study of microstrip plate geometries as UV photosensors with reflective photocathodes: Simulation," *IEEE Trans. Nucl. Sci.*, vol. 48, pp. 411–416, 2001.

[10] C. M. B. Monteiro, J. F. C. A. Veloso, D. S. A. P. Freitas, J. M. F. dos Santos, and C. A. N. Conde, "The gas proportional scintillation counter/microstrip gas chamber hybrid detector with argon filling," *Nucl. Instrum. Methods*, 2002.